

Polarized GPDs and structure functions of ρ meson

Bao-Dong Sun^{1,2,a} and Yu-Bing Dong^{1,2,3,b}

¹ Institute of High Energy Physics, Chinese Academy of Sciences, Beijing 100049, P. R. China

² School of Physics, University of Chinese Academy of Sciences, Beijing 100049, P. R. China

³ Theoretical Physics Center for Science Facilities (TPCSF), CAS, Beijing 100049, P. R. China

Received: date / Revised version: date

Abstract. The ρ meson polarized generalized parton distribution functions, its structure functions g_1 and g_2 and its axial form factors $\tilde{G}_{1,2}$ are studied based on a light-front quark model for the first time. Comparing our obtained moments of g_1 to lattice QCD calculation, we find that our results are reasonably consistent to the Lattice predictions.

PACS. 12.38.Lg – 13.60.Fz – 14.40.Be – 14.65.Bt

1 Introduction

It is believed that the generalized parton distributions (GPDs) of a system could be a powerful tool to understand its hadronic structure [1]. This is because GPDs naturally embody the information of both form factors (FFs) and parton distribution functions (PDFs) for the complicated system. They can provide the normal PDFs for the longitudinal parton distribution as well as the transverse information. Consequentially, GPDs display the unique properties to present a "three-dimensional (3D)" description for the transverse and longitudinal partonic degrees of freedom inside the system. Furthermore, it should be addressed that the physical meaning of the transverse distribution is more transparent when one goes to the impact parameter space [2,3,4]. Another important potential of GPDs is the information about how the orbital angular momentum contributes to the total spin of a hadron. We know that the sum rules proposed by Xiangdong Ji for a nucleon (spin-1/2) reveal the relation between GPDs and the spin carried by quarks and gluons [5,6]. For the spin-1 hadrons, such as deuteron and ρ meson, one may also reach similar relations. Meanwhile they provide some new structure functions which have no analogue to the case of spin-1/2 targets [7,8,9].

For a spin-1 target, its form factors relate to its GPDs through sum rules. Among the total 9 GPDs, 5 unpolarized and 4 polarized ones, the sum rules of the unpolarized GPDs can give the charge G_C , magnetic G_M , and quadrupole G_Q form factors. We have intensively studied those observables with a help of a light-front constituent quark model for the ρ meson phenomenologically [10],

where the ρ meson form factors $G_{C,M,Q}(Q^2)$, mean square charge radius, magnetic and quadrupole moments are calculated. Our obtained results are reasonably compatible with the previous model calculations and the experimental data [11,12,13]. Moreover, our calculated results for the first Mellin moments of the unpolarized GPDs H_1 and H_5 , which respectively correspond to the reduced matrix elements and to the structure functions of F_1 and b_1 (the tensor structure), are in a good agreement with the results from Lattice QCD calculation [14].

To account for a polarized target, we know that the spin-dependent structure functions $g_1(x)$ and $g_2(x)$ are defined by the decomposition of the imaginary part of the forward virtual Compton scattering amplitudes [7,15,16,17]. In the leading order (twist-2), the forward limit of the polarized GPD $\tilde{H}_1(x,0,0)$ is related to $g_1(x)$ [8,14]. It is believed that the g_1 gives the information of the polarized quark densities, namely, the probabilities to find a polarized quark (with longitudinal momentum fraction x) parallel or antiparallel to the polarization of the target [18,19]. In addition, the sum $g_T = g_1 + g_2$ involves the transverse spin density [18]. In general, the structure functions, g_2 , or g_T , also receive the contributions from a quark-gluon correlation which comes from the twist-3 operator [20]. Thus, they may give the information of the "high-twist effects" in a system. Many theoretical and experimental studies have been preformed for both g_1 and g_2 (see for example Refs. [21,22,23,24,25]) in the literature. More details can be found in recent review articles [26,27,28].

To our knowledge, the spin-dependent structure functions g_1 and g_2 of spin-1 hadrons, particular for the ρ meson, have been rarely studied theoretically. Since we have successfully studied the unpolarized GPDs of the ρ meson

^a sunbd@ihep.ac.cn

^b dongyb@ihep.ac.cn

with a help of a light-front quark model, we extend our approach to further calculate the polarized GPDs of the ρ meson, and try to obtain its $g_1(x)$ from the forward limit of the polarized GPDs $\tilde{H}_1(x, 0, 0)$. It is known that the spin structure function g_2 is usually related to g_1 according to the Wandzura and Wilczek relation [29]. However, as emphasized by Jaffe and Ji [15,16], g_2 is not solely determined by g_1 as Wandzura and Wilczek concluded. There are another twist-2 function (h_T) and a twist-3 term which may also have non-negligible contributions to g_2 (see Refs. [15,16,20]). In this work, however, only twist-2 operators are involved and we ignore h_T and twist-3 terms as many other theoretical calculations [20,21] did for simplicity.

In addition, the axial form factors for the spin-1 particle $\tilde{G}_{1,2}$ are seldom discussed due to no axial current in electromagnetic interaction. However, after taking into account of the electro-weak interaction which contains axial vector currents, the two form factors can be measured through the respond functions $W_{1,2,8}$ [30]. This phenomenon is similar to the nucleon (spin-1/2) case [31]. Therefore, the axial form factors become important when we study the electro-weak structure of the system, such as the parity violating in the electron-deuteron scattering [32]. Since the axial form factors relates to the sum rules of the polarized GPDs of the system, we may also estimate them according to our obtained polarized GPDs for the ρ meson.

This paper is organized as follows. In Section 2, the definition and sum rules of the polarized GPDs and the structure functions g_1 etc. are briefly presented. Moreover, the light-front quark model employed in this and our previous works are also shortly discussed in this section. In Section 3, the evolution for the spin structure function g_1 is discussed. Section 4 gives our numerical results for the polarized GPDs, the spin structure functions of g_1 and g_2 , and the axial form factors of the ρ meson. Section 5 is devoted for a short summary.

2 Polarized GPDs and our model

Fig. 1 illustrates the process we are considering. The notations are [10]

$$\begin{aligned} t &= \Delta^2 = (p' - p)^2 = (q - q')^2, \quad Q^2 = -q^2, \\ \xi &= -\frac{\Delta \cdot n}{2P \cdot n} = -\frac{\Delta^+}{2P^+}, \quad |\xi| = \frac{\Delta^+}{2P^+}, \quad (|\xi| \leq 1) \\ x &= \frac{k \cdot n}{P \cdot n} = \frac{k^+}{P^+}, \quad (-1 \leq x \leq 1), \end{aligned} \quad (1)$$

where p and p' are the 4-momenta of the incoming and outgoing ρ mesons, $P = (p' + p)/2$, $\Delta = p' - p$, n is a light-like 4-vector with $n^2 = 0$. Here q is the virtual photon momentum, and q' is treated as a real one.

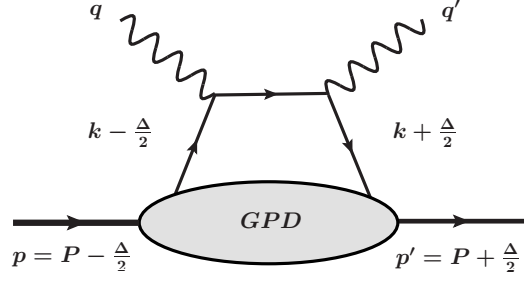


Fig. 1. The s-channel handbag diagram for GPDs. The u-channel one can be obtained by $q \leftrightarrow q'$.

The four polarized GPDs, for a spin-1 particle, are introduced in Ref. [8],

$$\begin{aligned} & \frac{1}{2} \int \frac{d\lambda}{2\pi} e^{ix(Pz)} \langle p' | \bar{q}(-\frac{1}{2}z) \not{n} \gamma_5 q(\frac{1}{2}z) | p \rangle \Big|_{z=\lambda n} \\ &= -i \frac{\epsilon_{\mu\alpha\beta\gamma} n^\mu \epsilon'^*{}^\alpha \epsilon^\beta P^\gamma}{Pn} \tilde{H}_1^q(x, \xi, t) \\ &+ 2i \frac{\epsilon_{\mu\alpha\beta\gamma} n^\mu \Delta^\alpha P^\beta}{Pn} \frac{\epsilon^\gamma(\epsilon'^* P) + \epsilon'^*{}^\gamma(\epsilon P)}{M^2} \tilde{H}_2^q(x, \xi, t) \\ &+ 2i \frac{\epsilon_{\mu\alpha\beta\gamma} n^\mu \Delta^\alpha P^\beta}{Pn} \frac{\epsilon^\gamma(\epsilon'^* P) - \epsilon'^*{}^\gamma(\epsilon P)}{M^2} \tilde{H}_3^q(x, \xi, t) \\ &+ \frac{i}{2} \frac{\epsilon_{\mu\alpha\beta\gamma} n^\mu \Delta^\alpha P^\beta}{Pn} \frac{\epsilon^\gamma(\epsilon'^* n) + \epsilon'^*{}^\gamma(\epsilon n)}{Pn} \tilde{H}_4^q(x, \xi, t) \end{aligned} \quad (2)$$

where $\epsilon_{0123} = 1$ and M is the ρ meson mass. Without loss of generality, we choose ρ^+ meson in this work and omit the superscript hereafter when there is no ambiguity. Thus, in the constituent quark model, only u and d contribute to the current operator in Eq. (2). In the equation, time reversal constraints that \tilde{H}_3^q are ξ -odd and all other GPDs ξ -even. Taking the lowest moments of the polarized GPDs in x , one recovers the axial vector form factors for each flavour q [8],

$$\int_{-1}^1 dx \tilde{H}_i^q(x, \xi, t) = \tilde{G}_i^q(t) \quad (i = 1, 2), \quad (3)$$

with matrix elements of

$$\begin{aligned} \langle p' | \bar{q}(0) \gamma^\mu \gamma_5 q(0) | p \rangle &= -2i \epsilon^\mu{}_{\alpha\beta\gamma} \epsilon'^*{}^\alpha \epsilon^\beta P^\gamma \tilde{G}_1^q(t) \\ &+ 4i \epsilon^\mu{}_{\alpha\beta\gamma} \Delta^\alpha P^\beta \frac{\epsilon^\gamma(\epsilon'^* P) + \epsilon'^*{}^\gamma(\epsilon P)}{M^2} \tilde{G}_2^q(t). \end{aligned} \quad (4)$$

For other two GPDs, time reversal invariance gives

$$\int_{-1}^1 dx \tilde{H}_3^q(x, \xi, t) = 0, \quad (5)$$

and the Lorenz invariance constraints

$$\int_{-1}^1 dx \tilde{H}_4^q(x, \xi, t) = 0. \quad (6)$$

Recall that the neutral current that couple to the Z boson is [33,34]

$$J_u^Z = \frac{1}{\cos\theta_w} (J_\mu^3 - \sin^2\theta_w J_\mu^{\text{EM}}) , \quad (7)$$

where θ_w is the weak mixing angle and the electromagnetic current for quarks

$$J_\mu^{\text{EM}} = +\frac{2}{3}\bar{u}\gamma^\mu u - \frac{1}{3}\bar{d}\gamma^\mu d - \frac{1}{3}\bar{s}\gamma^\mu s + \dots , \quad (8)$$

and

$$J_\mu^3 = \frac{1}{4} [\bar{u}\gamma^\mu(1-\gamma_5)u - \bar{d}\gamma^\mu(1-\gamma_5)d - \bar{s}\gamma^\mu(1-\gamma_5)s + \dots] , \quad (9)$$

where " \dots " represents heavy quarks, we get the axial vector form factors

$$\tilde{G}_i = \tilde{G}_i^u - \tilde{G}_i^d - \tilde{G}_i^s + \dots , (i = 1, 2) , \quad (10)$$

with the definition in Eq. (4). As shown later (in Eq. (18)), we see that under the isospin symmetry, $\tilde{G}_i^u = \tilde{G}_i^d$ in ρ^+ and the contributions of light u and d quarks to the total axial vector form factors cancel each other. When considering only the u and d flavours simultaneously, one gets $\tilde{G}_{1,2} = 0$ [30].

Due to the isospin symmetry and charge symmetry (G-parity), the polarized (or axial) GPDs are related by

$$\tilde{H}_{i,\rho^+}^u(x, \xi, t) = \tilde{H}_{i,\rho^+}^d(-x, \xi, t) , \quad (11)$$

where $i = 1 \sim 4$. Project the axial (polarized) GPDs onto isoscalar and isovector combinations, we have

$$\tilde{H}_i^{I=0}(x, \xi, t) = \frac{1}{2} [\tilde{H}_i^u(x, \xi, t) + \tilde{H}_i^d(x, \xi, t)] , \quad (12)$$

$$\tilde{H}_i^{I=1}(x, \xi, t) = \frac{1}{2} [\tilde{H}_i^u(x, \xi, t) - \tilde{H}_i^d(x, \xi, t)] , \quad (13)$$

and the corresponding axial vector isoscalar and isovector form factors are

$$\int_{-1}^1 dx \tilde{H}_i^{I=0}(x, \xi, t) = \tilde{G}_i^u(t) + \tilde{G}_i^d(t) \equiv \tilde{G}_i^{I=0}(t) , \quad (14)$$

$$\int_{-1}^1 dx \tilde{H}_i^{I=1}(x, \xi, t) = \tilde{G}_i^u(t) - \tilde{G}_i^d(t) \equiv \tilde{G}_i^{I=1}(t) . \quad (15)$$

With Eq. (11), one gets

$$\tilde{H}_i^{I=0}(x, \xi, t) = \tilde{H}_i^{I=0}(-x, \xi, t) , \quad (16)$$

$$\tilde{H}_i^{I=1}(x, \xi, t) = -\tilde{H}_i^{I=1}(-x, \xi, t) , \quad (17)$$

which give

$$\tilde{G}_i^{I=0}(t) = 2\tilde{G}_i^u(t) , \quad \tilde{G}_i^{I=1}(t) = 0 , \quad (i = 1, 2) , \quad (18)$$

This results from $\tilde{G}_i^u = \tilde{G}_i^d$ in ρ^+ .

For a comparison to the unpolarized case, we note that, for the unpolarized GPDs [10], there is an overall minus sign difference w.r.t. Eq. (11) and Eq. (13), respectively,

$$H_{i,\rho^+}^u(x, \xi, t) = -H_{i,\rho^+}^d(-x, \xi, t) , \quad (19)$$

$$H_{i,\rho^+}^{I=1}(x, \xi, t) = H_{i,\rho^+}^{I=1}(-x, \xi, t) . \quad (20)$$

where $i = 1 \sim 5$. More details on the projection are referred to Refs. [10,35,36].

As emphasized in Ref. [30], the axial vector form factors \tilde{G}_1 and \tilde{G}_2 are usually discarded in the previous studies. After considering the electro-weak interaction, one may expect nonzero strange quark contribution to \tilde{G}_1 and \tilde{G}_2 , by measuring the difference between the cross sections of the pure electromagnetic interaction and the electro-weak interaction. These measurements can provide an important probe for the electro-weak structure of the nucleons [32]. For the ρ meson, which is a isovector system, it is still quite interesting to know what these two form factors, for u and d flavours, look like under our phenomenological calculation.

In the forward limit $\Delta = 0$, only \tilde{H}_1^q survives and has quark density interpretation. Using the relation of the helicity amplitudes for finding a quark in a ρ meson [8], one gets

$$\tilde{H}_1^q(x, 0, 0) = q_\uparrow^1(x) - q_\downarrow^1(x) \equiv \Delta q(x) , \quad (21)$$

where $x > 0$ and $q_\uparrow^1(x)$ is the probability to find a quark with momentum fraction x and polarization parallel to the ρ meson helicity $+1$. Here $\Delta q(x)$ is called the spin dependent density [1], or the polarized quark distribution [6]. The parity constraints $q_\uparrow^1 = q_\downarrow^{-1}$. In the frame of GPDs, Eq. (21) with $x < 0$ stands for the antiquark (\bar{q}) distribution at $-x$. This leads to the partonic decomposition [1,6]

$$\tilde{H}_1^q(x, 0, 0) = \theta(x)\Delta q(x) + \theta(-x)\Delta\bar{q}(-x) . \quad (22)$$

By Eqs. (11) and (22), one gets

$$\Delta u_{\rho^+}(x) = \Delta\bar{d}_{\rho^+}(x) . \quad (23)$$

As discussed in Ref. [1], the x -even ("singlet") combination

$$\tilde{H}_1^{q(+)}(x, \xi, t) = \tilde{H}_1^{q(+)}(x, \xi, t) + \tilde{H}_1^{q(+)}(-x, \xi, t) \quad (24)$$

corresponds to the charge conjugation $C = +1$, and gives $\tilde{H}_1^{q(+)}(x, 0, 0) = \Delta q(x) + \Delta\bar{q}(x)$ in the forward limit. The x -odd ("nonsinglet" or "valence") combination

$$\tilde{H}_1^{q(-)}(x, \xi, t) = \tilde{H}_1^{q(+)}(x, \xi, t) - \tilde{H}_1^{q(+)}(-x, \xi, t) \quad (25)$$

corresponds to the charge conjugation $C = -1$, and gives $\tilde{H}_1^{q(-)}(x, 0, 0) = \Delta q(x) - \Delta\bar{q}(x)$ in the forward limit. Thus, like the pion case [36,37], for ρ^+ , the valence (or nonsinglet) polarized quark distribution is

$$\tilde{V} = \Delta u_\rho - \Delta\bar{u}_\rho + \Delta\bar{d}_\rho - \Delta d_\rho , \quad (26)$$

and the singlet polarized quark distribution is

$$\tilde{S} = \Delta u_\rho + \Delta \bar{u}_\rho + \Delta d_\rho + \Delta \bar{d}_\rho + \Delta s_\rho + \Delta \bar{s}_\rho. \quad (27)$$

These two combinations do not mix under evolution (see Sec. 3). The sea-quark distribution is defined as [37]

$$\tilde{s} = \tilde{S} - \tilde{V} = 2(\Delta \bar{u}_\rho + \Delta d_\rho) + \Delta s_\rho + \Delta \bar{s}_\rho. \quad (28)$$

In the present work, ρ^+ meson is restricted to be only composed by an active quark u and an active antiquark \bar{d} , which means the contribution of sea quarks (\bar{u} , d , s and \bar{s}) is not included here.

On the other hand, at leading order, the polarized structure function $g_1^q(x)$ gives the fraction of spin carried by quarks [14]

$$g_1^q(x) = \frac{1}{2} [q_\uparrow^1(x) - q_\downarrow^1(x)] + \{q \rightarrow \bar{q}\}, \quad (29)$$

and follows the relation [8, 14]

$$g_1(x) = \sum_q e_q^2 g_1^q(x). \quad (30)$$

Therefore, with Eqs. (21) and (23), we get

$$g_1(x) = \frac{1}{2} e_u^2 \Delta u(x) + \frac{1}{2} e_{\bar{d}}^2 \Delta \bar{d}(x) = \frac{1}{2} (e_u^2 + e_{\bar{d}}^2) \Delta u(x) \quad (31)$$

$$\Delta q \equiv \int_0^1 [g_1^u(x) + g_1^{\bar{d}}(x)] dx = \int_0^1 \Delta u(x) dx. \quad (32)$$

where Δq is the total fraction of spin carried by valence u and \bar{d} in ρ^+ .

In general, the rigorous expression for the structure function g_2 contains another twist-2 piece, "transversity" h_T , and a twist-3 piece arising from quark-gluon correlation [20, 21]. h_T is proportional to the ratio of the current quark mass to the target mass ($\sim m_c/M$) and it is commonly neglected in most studies [21]. In present work, both h_T and the twist-3 parts are neglected, although it may not be small. Under those approximation, one gets the Wandzura-Wilczek relation [29] for g_2 ,

$$g_2^{WW}(x) = -g_1(x) + \int_x^1 \frac{dy}{y} g_1(y). \quad (33)$$

Here, the Q^2 -dependence is ignored, since at large Q^2 , the g_1 and g_2 become scalling. It may not be a good approximation to identify $g_2(x) = g_2^{WW}(x)$ (which may have 15 ~ 40% breaking of the size of g_2 [38]), however, we argue that it, at least, allows us to estimate the contribution of the axial current operator to g_2 . In this case, it is easy to verify the Burkhardt-Cottingham sum rule [39] by changing the integral variables,

$$\int_0^1 g_2(x) dx = 0. \quad (34)$$

Notes that, according to Ref. [15], this relation remains to be tested since the derivation in [39] is based on the assumption of the Regge theory. However, Ref. [21] claims,

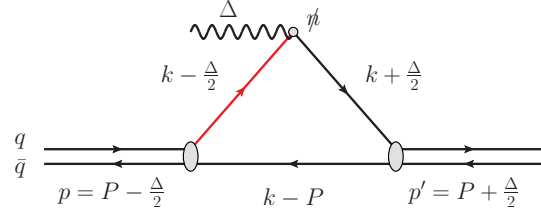


Fig. 2. The struck u quark in the valence regime. The momentum of the red line have positive plus component.

for proton, this sum rule for g_2 holds up to order $O(M^2/Q^2)$. Finally, with those approximations, one gets the transverse spin density [18, 29]

$$g_T(x) = g_1(x) + g_2(x) \sim \int_x^1 \frac{dy}{y} g_1(y).$$

The Mellin moment of a function $f(x)$ is defined as

$$M_n(f) = \int_0^1 x^{n-1} f(x) dx. \quad (35)$$

For the ρ meson case, at the leading order (twist 2), one finds [14]

$$2M_n(g_1^q) = C_n^{(1)} r_n, \quad (36)$$

where $C_n^{(k)} = 1 + O(\alpha)$ is the Wilson coefficient of the operator product expansion and r_n are the reduced matrix elements. These relations hold for both even and odd n th orders with the quenched approximation. Notes that there are two different sets of notations labeling the moments of F_1 , b_1 and g_1 respectively in Refs. [14] and [19]. Here we follow the former.

In a numerical calculation, we employ our phenomenological light-front quark model to describe the interaction between the spin-1 ρ meson and its constituents u and \bar{d} . It is based on an effective interaction Lagrangian for the $\rho \rightarrow \bar{q}q$ vertex,

$$\begin{aligned} \mathcal{L}_I &= -\frac{iM}{f_\rho} \bar{q} \Gamma^\mu \tau q \cdot \rho_\mu \\ &= -\frac{i\sqrt{2}M}{f_\rho} \left[\frac{\bar{u} \Gamma^\mu u - \bar{d} \Gamma^\mu d}{\sqrt{2}} \rho_\mu^0 + \bar{u} \Gamma^\mu d \rho_\mu^+ + \bar{d} \Gamma^\mu u \rho_\mu^- \right], \end{aligned} \quad (37)$$

where ρ_μ is the ρ meson field, f_ρ is the ρ decay constant (which may be absorbed in the normalization factor N), and Γ^μ is a Bethe-Salpeter amplitude (BSA) [10, 40],

$$\Gamma^\mu = N \frac{\gamma^\mu - (k_q + k_{\bar{q}})^\mu / (M_{i,f} + 2m)}{[k_q^2 - m_R^2 + i\epsilon][k_{\bar{q}}^2 - m_R^2 + i\epsilon]}, \quad (39)$$

where, for the u quark contribution, the struck u quark momentum $k_u = k - \Delta/2$ and the spectator constituent momentum is $k_s = k_{\bar{d}} = k - P$, as shown in Fig. 2. N is the normalization constant, m and m_R are the constituent

quark and the regulator masses, respectively, and $M_{i,f}$ are the kinematic invariant masses, [10,40]

$$M_i^2 = \frac{\kappa_\perp^2 + m^2}{1 - x'} + \frac{\kappa'_\perp^2 + m^2}{x'}, \quad (40)$$

$$M_f^2 = \frac{\kappa_\perp'^2 + m^2}{1 - x''} + \frac{\kappa_\perp^2 + m^2}{x''}, \quad (41)$$

where the subscript $i(f)$ for initial(final) state and, following momenta convention in Fig. 2, the LF momentum fractions $x'(x'')$ and $\kappa_\perp(\kappa'_\perp)$ are

$$x' = -\frac{k_s^+}{p^+} = \frac{1 - x}{1 - |\xi|}, \quad x'' = x' \frac{p^+}{p'^+} = \frac{1 - x}{1 + |\xi|},$$

$$\kappa_\perp = (k - P)_\perp - \frac{x'}{2} \Delta_\perp, \quad \kappa'_\perp = (k - P)_\perp + \frac{x''}{2} \Delta_\perp \quad (42)$$

In the nonvalence regime where $-|\xi| < x < |\xi|$ leads to $x' > 1$ in Eq. (40), and the initial vertex becomes the non-wave-function vertex. To keep the mass square positive, as Refs. [10,40], we directly replace $1 - x'$ with $x' - 1$ in Eq. (40) and get

$$M_{i(NV)}^2 = \frac{\kappa_\perp^2 + m^2}{x' - 1} + \frac{\kappa'_\perp^2 + m^2}{x'}. \quad (43)$$

Here, to keep this phenomenological Γ^μ respecting to the isospin symmetry (which is required by Eqs. (11), (19) and (23)), one has to employ the symmetric momenta convention as shown in Fig. 2. More details are explained in our previous work [10].

3 On the QCD Evolution

Comparing the model-dependent results to the available "data", like the Lattice QCD calculation, one may perform a QCD evolution to evolve the parton distribution and its moments from the factorization scale μ_0 to the scale that a Lattice QCD calculation is performed. For the calculated ρ meson polarized GPDs or structure functions in the present work, we compare our result with lattice QCD results at the scale $\mu = 2.4\text{GeV}$ with quenched approximation [14], as our previous work for the unpolarized ones. Here, we ignore the gluon contribution to the evolution, thus, we can adopt the same (LO) DGLAP evolution function for the moments of the single flavor structure function $g_1^u(x)$ as

$$\frac{\tilde{V}_n^u(\mu)}{\tilde{V}_n^u(\mu_0)} = \left(\frac{\alpha(\mu)}{\alpha(\mu_0)} \right)^{\gamma_n^{(0)}/(2\beta_0)}, \quad (44)$$

where the single quark spin fractions

$$\tilde{V}_n^u = 2M_{n+1} [g_1^u(x)] \sim r_{n+1}$$

and the running coupling constant is

$$\alpha(\mu) = \frac{4\pi}{\beta_0 \log(\mu^2/\Lambda_{QCD}^2)}, \quad (45)$$

where $\beta_0 = 11N_c/3 - 2N_f/3$ with $N_c = N_f = 3$ and

$$\Lambda_{QCD} = 0.226 \text{ GeV} \quad (46)$$

being employed [37,41]. In our previous work, we performed the evolution of the Mellin moments of unpolarized structure function, and found the factorization scale of the model is $\mu_0 = 528_{-62}^{+77} \text{ MeV}$.

In our previous work, we obtained the evolution ratio for the valence quark distribution, by calculating the evolution of the active u quark unpolarized distribution. Here we adopt the same ratio for the evolution of valence polarized quark distribution (or their Mellin moments) to compare with the Lattice QCD results, since the scale $\mu = 2.4\text{GeV}$ is same for both unpolarized and polarized cases. In addition, the sea quark contributions (Eq. (28)) are excluded from our calculation, thus one can observe that the nonsinglet (Eq. (26)) and singlet (Eq. (27)) polarized quark distributions make no more difference in present work.

4 Numerical results

Following our previous work on the unpolarized GPDs [10], we take the two model parameters, the constituent mass $m = 0.403 \text{ GeV}$ and regulator mass $m_R = 1.61 \text{ GeV}$. We simply extend the model to the polarized GPDs $\tilde{H}_{1,2}$ case. Their x - and t -dependences with skewness $\xi = 0$ and $\xi = -0.4$ are shown in Fig. 3 and in Fig. 4 respectively. The results are normalized with respect to the corresponding u quark axial form factors. The obtained polarized GPDs are displayed with opposite values between the regions $[-1, 0]$ and $[0, 1]$, as a consequence of the isospin symmetry of our model. At the joint points of valence and non-valence regions, namely at $|x| = |\xi| = 0.4$ in Figs. 3(b) and 4(b), our resulted $\tilde{H}_{1,2}$ are continuous. This phenomenon fulfills the requirement of the consistency of factorization at leading twist [1]. Here, we take the momentum transfer t up to -10 GeV^2 , similar to the unpolarized case. Comparing to the unpolarized GPDs, especially H_1 , we find that the polarized GPDs $\tilde{H}_{1,2}$ vary much slow with respect to t . Figs. 5 and 6 show the single flavour axial form factor $\tilde{G}_1^u(t)$ and $\tilde{G}_2^u(t)$, respectively. Within the region $-10 \text{ GeV}^2 < t < 0$, $\tilde{G}_1^u(t)$ is larger than $\tilde{G}_2^u(t)$ and decreases slower than $\tilde{G}_2^u(t)$ as t increases. The starting points is $\tilde{G}_1^u(0) = 0.86$ and $\tilde{G}_2^u(0) = -0.16$, respectively. Correspondingly, we have $\tilde{G}_1^{I=0}(0) = 1.72$ and $\tilde{G}_2^{I=0}(0) = -0.32$, respectively.

In Fig. 7 and Fig. 8, the x dependence of g_1^u and g_2^u are shown. Our result for $g_1^u(x)$ remains positive in the whole $0 < x < 1$ region and it is nearly symmetry around $x = 1/2$. The available experimental data for deuteron $g_1^{(d)}(x)$, summarized in Ref. [24], have negative values at small x region, but it is believed to be consistent with zero after combining the new COMPASS result [25]. We

think our result for the ρ meson may indirectly confirm the positiveness of $g_1(x)$. In general, our twist-2 results for the ρ meson g_1 have similar x -dependence behavior with the g_1 of the deuteron in the new COMPASS result [25] (see its Fig. 4). Summing over x of $g_1^u(x) + g_1^d(x)$ as Eq. (32), we get

$$\Delta q = 0.86 . \quad (47)$$

which means the fraction of spin carried by constituent quark and antiquark in ρ meson is 0.86, while the expected value is 1. This result is similar to the case of the nucleon (see for example Ref. [42]). In general, the total fraction of spin carried by quarks and antiquarks in nucleon is not more than 30% to 50%. It is well known as the ‘‘spin crisis’’ issue (or ‘‘spin puzzle’’) [6, 26, 28, 42]. As proposed by Sehgal [43], another important contribution to the proton spin may come from the orbital angular momentum of partons. Through the light-cone representation of the spin and orbital angular momentum of relativistic composite systems, Brodsky, Hwang, Ma and Schmidt [44] have shown that the ‘‘spin crisis’’ of the nucleon can be explained due to the relativistic motion of quarks, and the contribution of the orbital angular momentum. Thus the small Δq can be naturally understood. According to Myhrer, Bass and Thomas etc [45, 46], the nucleon ‘‘spin crisis’’ maybe also be understood through the pion cloud effect together with relativistic corrections and one-gluon exchange, which can transfer the quark spin to the orbital angular momentum and it mainly accounts for the missing spin. The pions play a role of quark and antiquark sea. Here, we suggest that the orbital angular momentum may also be an important source for ρ meson spin and the corresponding parton splitting processes $q \rightarrow qq$ and $g \rightarrow q\bar{q}$ responsible for the DGLAP evolution, generate the orbital angular momentum [1]. After the evolution to a higher scale $\mu = 2.4$ GeV, as r_1 shown in Fig. (10) later, Δq becomes to around 60%.

Another way to understand the proton spin problem (see for example Refs. [47, 48]) is to consider the Wigner rotation of the spin of a moving quark. In this sense, there is no need to require the sum of quark’s spin equals to the total proton spin in light front frame.

For the $g_2(x)$ structure function, the present constituent model predicts that

$$\int_0^1 g_2(x) dx = 0.000112 , \quad (48)$$

comparing with the Burkhardt-Cottingham sum rule Eq. (34), we conclude that it is numerically consistent with vanishing. With Eq. (34), we find that $g_2(x)$ has a remarkable feature of a nontrivial zero apart from $x = 0$ and $x = 1$. Note again that g_2 should also receive contributions from twist-3 quark-gluon correlation which may be not small comparing to that of the twist-2 piece. The importance of this unique feature has stressed in previous works [16, 20, 23].

If one takes the massless limit of quark (asymptotic free), then $g_T = g_1 + g_2$ would be small, but this phenomenon contradicts to the ρ meson rest mass, since the quarks are not free inside hadrons, especially in the constituent quark model. Our results (see Fig. 7) tell that g_T^u is sizeable in the small and moderate x regions (< 0.5) and becomes much smaller in large x region. It may be interpreted that as the quark possesses more fraction of longitudinal momentum (larger x), it contributes less to the transverse spin density.

The numerical evolution for the polarized structure functions is similar to the unpolarized case. With the similar ratio, which is 0.67, we evolve our results for the moments of g_1 to the scale of Lattice QCD result [14]. We compare the results of the two approaches in Fig. 10. The results of r_n in Ref. [14] was obtained with two sets of operators, and in Fig. 10 we plot their averaged values. In general, our results agree with the Lattice QCD ones. Moreover, one more order of the moment (see r_4) is given by our calculation.

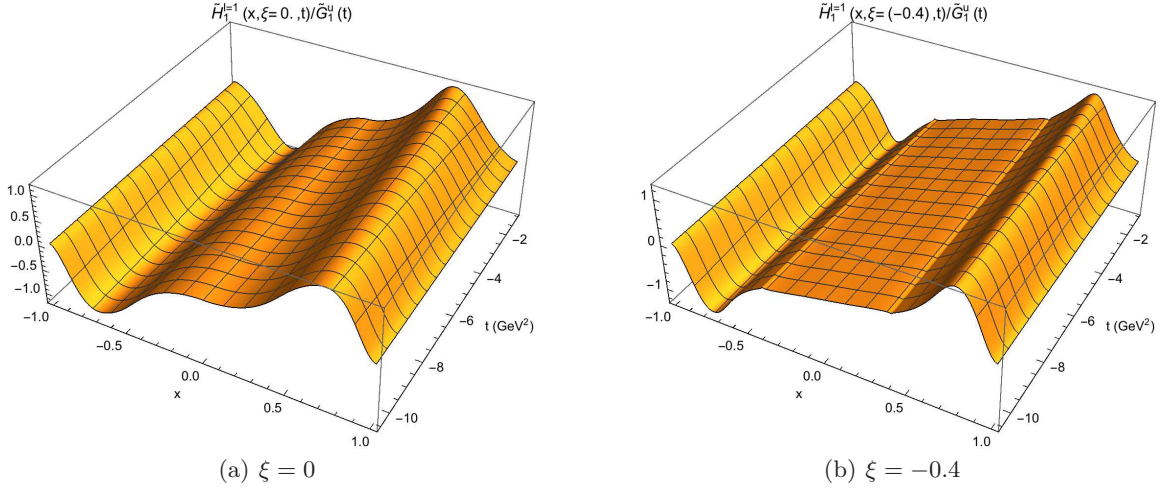
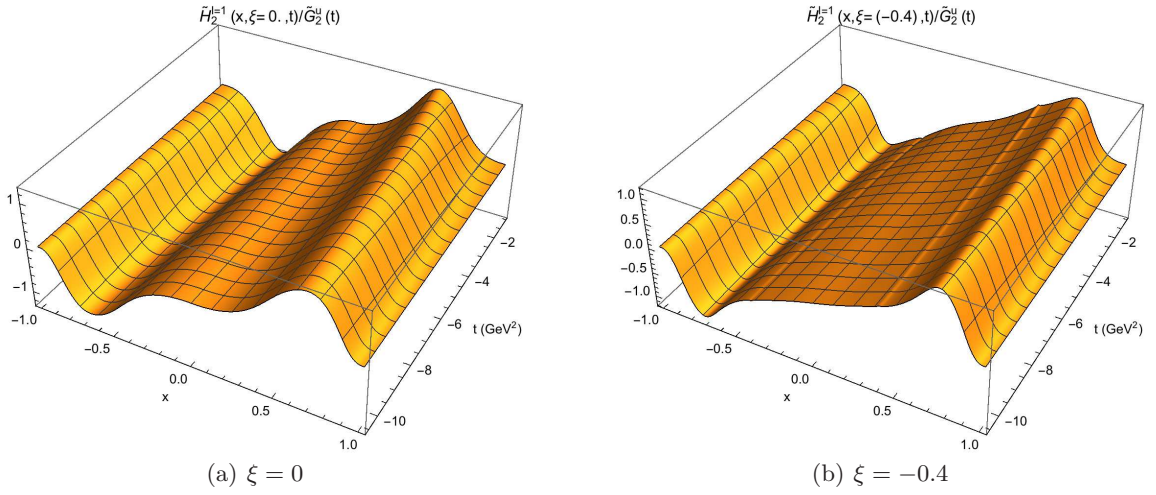
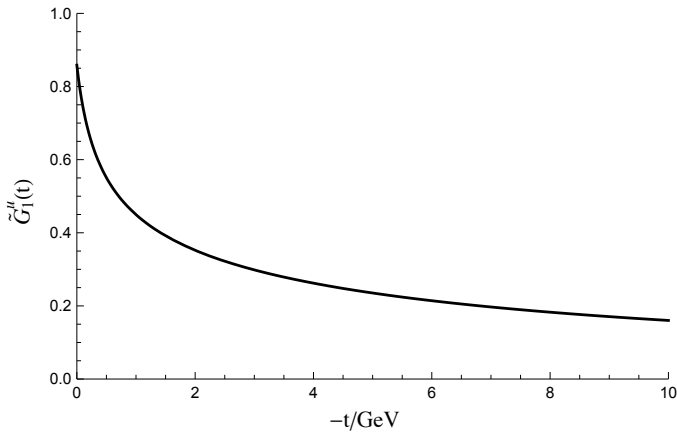
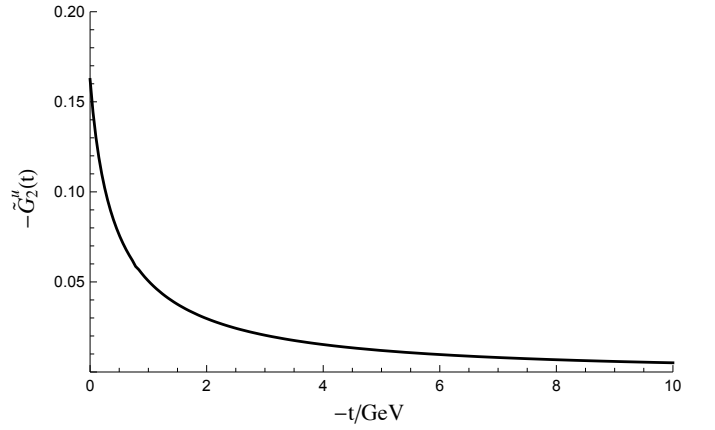
5 Conclusions

In this work, we extend our previous work on the ρ meson GPDs with light-front constituent quark model to the polarized case. The polarized GPDs $\tilde{H}_{1,2}$ with nonzero skewness (e.g. $\xi = -0.4$) are given in 3-D plot w.r.t. x and t . With the sum rules for $\tilde{H}_{1,2}$, we obtained its axial form factors $\tilde{G}_{1,2}$, the spin structure functions $g_1(x)$ and $g_2(x)$, and the moments for $g_1(x)$. After the evolution, our results of the moments of g_1 agree with the Lattice QCD results. The quark spin contribution ($\Delta q = 0.86$) to the ρ meson spin and the transverse spin density g_T for the ρ meson are also estimated with the constituent quark model for the first time. The small value of Δq for ρ may be mainly explained by its transfer to the orbital angular momentum carried by valence quarks, which is also a possible resolution of the nucleon spin problem. Our numerical result for $g_2(x)$ shows that the Burkhardt-Cottingham sum rule holds reasonably well in this work.

This work is supported by the National Natural Science Foundation of China under Grant No. 11475192, by the fund provided to the Sino-German CRC 110 ‘‘Symmetries and the Emergence of Structure in QCD’’ project by the NSFC under Grant No.11621131001, and the Key Research Program of Frontier Sciences, CAS, Grant No. Y7292610K1.

References

1. M. Diehl, Phys. Rept. **388**, 41 (2003).
2. M. Burkardt, Int. J. Mod. Phys. A **18**, 173 (2003).
3. G.A. Miller, Ann. Rev. Nucl. Part. Sci. **60**, 1 (2010).
4. B.-D. Sun, Y.-B. Dong, Chin. Phys. C **42**(6), 063104 (2018).
5. X.D. Ji, Phys. Rev. D **55**, 7114 (1997).
6. X.D. Ji, J. Phys. G **24**, 1181 (1998).


Fig. 3. ρ^+ GPD \tilde{H}_1 with $\xi = 0$ and -0.4 .

Fig. 4. ρ^+ GPD \tilde{H}_2 with $\xi = 0$ and -0.4 .

Fig. 5. The u quark axial form factor $\tilde{G}_1^u(t)$.

Fig. 6. The u quark axial form factor $\tilde{G}_2^u(t)$

 7. P. Hoodbhoy, R.L. Jaffe, A. Manohar, Nucl. Phys. B **312**, 571 (1989).

 8. E.R. Berger, F. Cano, M. Diehl, B. Pire, Phys. Rev. Lett. **87**, 142302 (2001).

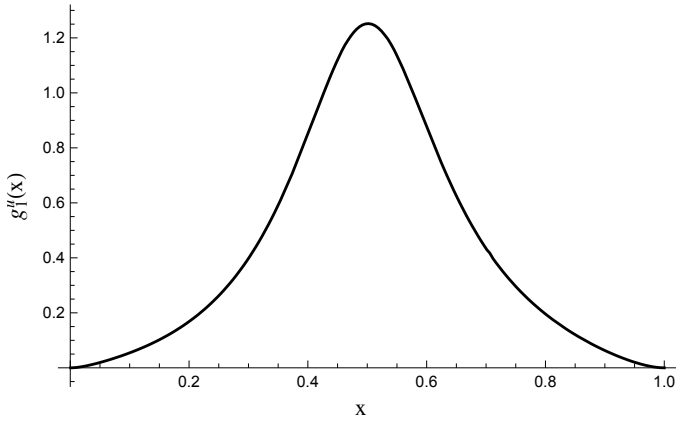


Fig. 7. The u quark structure function $g_1^u(x)$

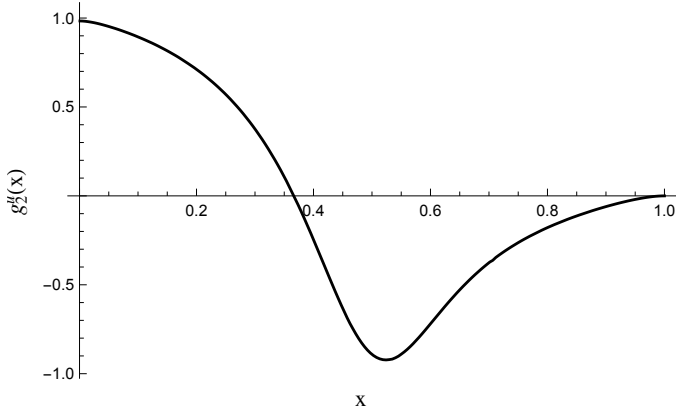


Fig. 8. The u quark structure function $g_2^u(x)$

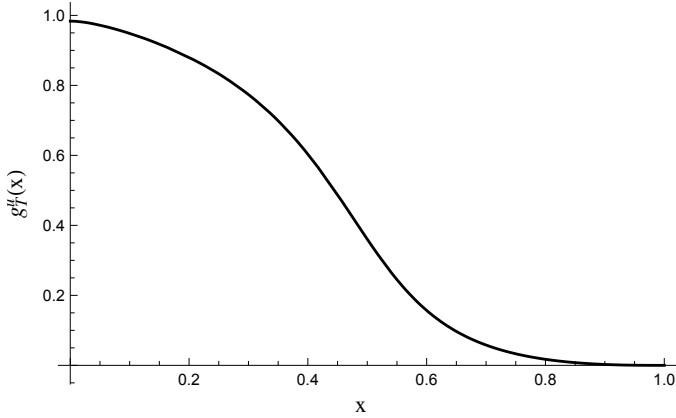


Fig. 9. $g_T^u(x)$

9. W. Cosyn, Y.-B. Dong, S. Kumano, M. Sargsian, Phys. Rev. D **95**(7), 074036 (2017).
10. B.-D. Sun, Y.-B. Dong, Phys. Rev. D **96**(3), 036019 (2017).
11. J.P.B.C. de Melo, T. Frederico, Phys. Rev. C **55**, 2043 (1997).
12. D. Garcia Gudino, G. Toledo Schnchez, Int. J. Mod. Phys. Conf. Ser. **35**, 1460463 (2014).
13. A.F. Krutov, R.G. Polezhaev, V.E. Troitsky, Phys. Rev. D **97**(3), 033007 (2018).
14. C. Best et al., Phys. Rev. D **56**, 2743 (1997).

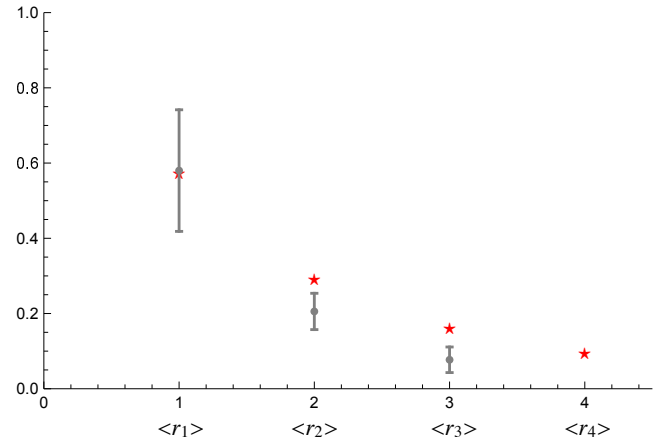


Fig. 10. r_n for u quark. The red stars are our results and the gray ones with errors are the Lattice QCD results [14].

15. R.L. Jaffe, Comments Nucl. Part. Phys. **19**(5), 239 (1990).
16. R.L. Jaffe, X.D. Ji, Phys. Rev. D **43**, 724 (1990)
17. P.A.M. Guichon, M. Vanderhaeghen, Prog. Part. Nucl. Phys. **41**, 125 (1998).
18. R.P. Feynman, *Photon-hadron interactions* (Benjamin Press, New York 1972) 132-159.
19. L. Mankiewicz, Z. Ryzak, Phys. Rev. D **43**, 733 (1991), .
20. J.L. Cortes, B. Pire, J.P. Ralston, Z. Phys. C **55**, 409 (1992).
21. X. Song, Phys. Rev. D **54**, 1955 (1996).
22. Y.-B. Dong, Phys. Lett. B **408**, 393 (1997).
23. P.L. Anthony et al., Phys. Lett. B **458**, 529 (1999), *ibid.* **553**, 18 (2003).
24. A. Airapetian et al., Phys. Rev. D **75**, 012007 (2007).
25. C. Adolph et al., Phys. Lett. B **769**, 34 (2017).
26. S.E. Kuhn, J.-P. Chen, E. Leader, Prog. Part. Nucl. Phys. **63**, 1 (2009).
27. J. P. Chen, Int. J. Mod. Phys. E **19**, 1893 (2010).
28. C.A. Aidala, S.D. Bass, D. Hasch, G.K. Mallot, Rev. Mod. Phys. **85**, 655 (2013).
29. S. Wandzura, F. Wilczek, Phys. Lett. B **72**, 195 (1977).
30. S.J. Pollock, Phys. Rev. D **42**, 3010 (1990), *ibid.* **43**, 2447 (1991).
31. D.B. Kaplan, A. Manohar, Nucl. Phys. B **310**, 527 (1988).
32. T.M. Ito et al., Phys. Rev. Lett. **92**, 102003 (2004).
33. M.J. Musolf et al., Phys. Rept. **239**, 1 (1994).
34. M.D. Schwartz, *Quantum Field Theory and the Standard Model* (Cambridge University Press, New York 2014) 592-595.
35. T. Frederico, E. Pace, B. Pasquini, G. Salme, Phys. Rev. D **80**, 054021 (2009).
36. M.V. Polyakov, C. Weiss, Phys. Rev. D **60**, 114017 (1999).
37. W. Broniowski, E.R. Arriola, K. Golec-Biernat, Phys. Rev. D **77**, 034023 (2008).
38. A. Accardi, A. Bacchetta, W. Melnitchouk, M. Schlegel, JHEP **11**, 093 (2009).
39. H. Burkhardt, W.N. Cottingham, Annals Phys. **56**, 453 (1970).
40. H.-M. Choi, C.-R. Ji, Phys. Rev. D **70**, 053015 (2004).
41. W. Broniowski, E.R. Arriola, Phys. Rev. D **78**, 094011 (2008).
42. A. Deur, S. J. Brodsky, G.F. De Tramond, arXiv:1807.05250.

- 43. L.M. Sehgal, Phys. Rev. D **10**, 1663 (1974), *ibid.* **11**, 2016 (1975).
- 44. S. J. Brodsky, D. S. Hwang, B. Q. Ma, I. Schmidt, Nucl. Phys. B **593**, 311 (2001).
- 45. A.W. Schreiber, A.W. Thomas, Phys. Lett. B **215**, 141 (1988).
- 46. F. Myhrer, A.W. Thomas, Phys. Lett. B **663**, 302 (2008).
- 47. B.Q. Ma, J. Phys. G **17**, L53 (1991).
- 48. B.Q. Ma, Q.R. Zhang, Z. Phys. C **58**, 479 (1993).

